

MicroRNA-18a-5p regulates the Warburg effect by targeting hypoxia-inducible factor 1 α in the K562/ADM cell line

KUN WU¹⁻³, CHONG GUO¹⁻³, YIXUN LI¹⁻³, JINRONG YANG^{4,5}, QIANG ZHOU^{4,5}, SHENJU CHENG¹⁻³, YANHONG LI¹⁻³, BO NIE^{4,5} and YUN ZENG^{4,5}

¹Department of Clinical Laboratory; ²Yunnan Key Laboratory of Laboratory Medicine; ³Yunnan Innovation Team of Clinical Laboratory and Diagnosis; ⁴Department of Hematology; ⁵Hematology Research Center of Yunnan Province, The First Affiliated Hospital of Kunming Medical University, Kunming, Yunnan 650032, P.R. China

Received March 22, 2020; Accepted February 2, 2021

DOI: 10.3892/etm.2021.10503

Abstract. The Warburg effect is involved in drug resistance and recurrence of cancer, and poses a challenge for the treatment of chronic myelogenous leukemia (CML). Hypoxia-inducible factor 1 α (HIF-1 α) plays a key role in the Warburg effect. microRNAs (miRs) targeting HIF-1 α have potential of regulating such aberrant metabolic process. The present study demonstrated that miR-18a-5p was expressed at a low level in K562/ADM cells via reverse transcription-quantitative PCR (RT-qPCR). The results of the luciferase reporter assay indicated that miR-18a-5p could specifically bind the 3'-untranslated region of HIF-1 α . Through RT-qPCR and western blotting, it was revealed that miR-18a-5p downregulated the expression of HIF-1 α . By inhibiting HIF-1 α , miR-18a-5p suppressed aerobic glycolysis in K562/ADM cells, according to the results produced by glucose uptake, lactate production, pyruvate level and ATP synthesis measurement, along with the results obtained from extracellular acidification rate and oxygen consumption rate assays. These results provided new evidence that miR-18a-5p may suppress the Warburg effect by targeting HIF-1 α . Furthermore, via CCK-8 and flow cytometry assays, cells transfected with miR-18a-5p mimics were more sensitive to Adriamycin (AMD) compared with AMD group. Reversing the Warburg effect by miR-30a-5p might provide a potential therapeutic strategy for CML.

Introduction

Leukemia is a common hematological malignant tumor with an incidence rate of 5-8/100,000 per year, endangering human health and life. Chronic myelogenous leukemia (CML) represents one type of leukemia caused by the dysfunction of pluripotent hematopoietic cells in patients resulting in indefinite proliferation of these cells. The development of CML can be divided into chronic, accelerated and acute phases, with a slow progression in the early stage (1). Although treatments such as chemotherapy, interferon therapy and targeted therapy have progressed in recent years, multiple drug resistance (MDR) and relapse still constitute major challenges for curing CML (2). For example, MDR CML is highly resistant to chemotherapeutic drugs (3,4). Some patients can gradually become resistant to imatinib which is a tyrosine kinase inhibitor targeting the Bcr-Abl gene (5). New mechanisms associated with MDR have been found and further investigated in recent years (6), such as autophagy (7) and the Warburg effect (8), providing novel therapeutic targets for CML.

The Warburg effect, which is also called aerobic glycolysis, is an aberrant metabolic process during which glycolysis occurs in cancer cells even in the presence of oxygen. Cancer cells with the Warburg effect exhibit higher glucose uptake and lactate generation (9,10). It has been increasingly recognized that the Warburg effect plays an important role in drug resistance and can be utilized as a potential target for drug development (11,12). The Warburg effect has been reported in different types of cancer, including hepatic carcinoma (13), breast cancer (14), esophageal cancer (15) and leukemia. It has been demonstrated that glucose transporter-1 protein (GLUT) is upregulated and the level of lactate is elevated in pediatric acute lymphoblastic leukemia cells and that these cells are sensitive to glycolytic inhibitors (16). GLUT expression on the surface of Bcr-Abl-positive CML cells can be repressed by imatinib, resulting in decreased glucose uptake (17). Targeting the Warburg effect provides potential therapeutic opportunities for leukemia (18). A clinical trial has been carried out to change the metabolic process in order to enhance drug sensitivity (19). Hypoxia-inducible factor 1 α (HIF-1 α) plays a key role in the Warburg effect. Glycolytic gene expression can be enhanced by HIF-1 α through interaction with hypoxia-responsive

Correspondence to: Professor Yun Zeng, Department of Hematology, The First Affiliated Hospital of Kunming Medical University, 295 Xichang Road, Kunming, Yunnan 650032, P.R. China
E-mail: zengyun_fyy@sina.com

Professor Kun Wu, Department of Clinical Laboratory, The First Affiliated Hospital of Kunming Medical University, 295 Xichang Road, Kunming, Yunnan 650032, P.R. China
E-mail: wukunnana@sina.com

Key words: microRNA-18a-5, hypoxia-inducible factor 1 α , chronic myelogenous leukemia

elements of glycolytic gene promoters (20). In addition, overexpression of HIF-1 α is closely associated with cancer cell proliferation, apoptosis inhibition, cancer cell infiltration and MDR. Activation of HIF-1 α usually indicates poor prognosis of patients with tumors (21). The current study hypothesized that inhibiting HIF-1 α in leukemia cells, such as the Adriamycin-resistant CML cell line K562/ADM, may reverse the Warburg effect and improve drug sensitivity.

MicroRNAs (miRNAs/miRs) are short non-coding RNAs with a length of 20-25 nt that participate in regulating various biological effects, such as proliferation, apoptosis and invasion of cancer cells. It has been increasingly demonstrated that miRNAs play regulatory roles in different types of cancer (22,23). miRNAs constitute potential candidates for leukemia diagnosis and therapy (24). miR-18a-5p belongs to the miR-17-92 family (25). Aberrant expression of miR-18a-5p has been reported in esophageal squamous cell carcinoma, pancreatic cancer and thyroid cancer, and miR-18a-5p may function as an oncogene or a tumor suppressor (26,27). Previous studies mainly focused on the impact of miR-18a-5p on proliferation, apoptosis, invasion and migration of cancer cell (28,29). The present study aimed to explore the regulatory role of miR-18a-5p in the Warburg effect in K562/ADM cells, which will provide new insight into the mechanism of miR-18a-5p regulation in leukemia cells and potential targets for CML treatment.

Materials and methods

Materials. RPMI-1640 medium was from Hyclone; Cytiva. FBS, trypsin and penicillin-streptomycin solution were from Thermo Fisher Scientific, Inc. Chronic myelogenous leukaemia cell lines K562 and K562/ADM were from American Type Culture Collection. Primary human normal lymphocyte culture was kindly supplied by Dr Shaohua Wang from the Department of Pharmacology at the Medical School of Southeast University and maintained at the Department of Clinical Laboratory in The First Affiliated Hospital of Kunming Medical University. Cell Counting Kit-8 (CCK-8) reagent was from Dojindo Molecular Technologies, Inc. Adriamycin was from Sigma-Aldrich; Merck KGaA. K562/ADM cells were treated with 5 μ g/ml Adriamycin and incubated at 37°C with 5% CO₂ for 48 h. The coding sequence of HIF-1 α (National Center for Biotechnology Information reference sequence, NM_001530.3), HIF-1 α small interfering RNA (siHIF-1 α : 5'-CTACTCAGGACACAGATTTAGACTTGGAG-3') and the scramble siRNA (5'-CATCCTGAACAGACTTAAGACGTGGTAGT-3') were synthesized and cloned into pcDNA-3.1 vectors for HIF-1 α overexpression and knockdown by Sangon Biotech Co., Ltd. miRNAs that could specifically target HIF-1 α were screened using Targetscan 7.2 (http://www.targetscan.org/vert_72/) and Miranda 2.0 (<http://www.miranda.org/>) software. miR-18a-5p mimics (5'-GAUAGACGUGAUCUACGUGGAU-3') and miRNA negative control (miR-NC, 5'-UUCUCCGAACGUGUCACGUACG-3') were synthesized by Sangon Biotech Co., Ltd. Lipofectamine[®] 2000 was from Invitrogen; Thermo Fisher Scientific, Inc. RNAiso Plus[™] was from Takara Biotechnology Co., Ltd. RevertAid[™] Reverse Transcriptase was from Thermo Fisher Scientific, Inc. All reverse transcription-quantitative PCR (RT-qPCR) primers

were synthesized by Sangon Biotech Co., Ltd. miRNA qPCR Master Mix for miRNA quantification and 2X SGExcel FastSYBR Mixture for mRNA quantification were from Sangon Biotech Co., Ltd. HIF-1 α , glucose transporter type 1 (GLUT1), hexokinase 2 (HK2), pyruvate kinase M2 (PKM2), lactate dehydrogenase A (LDHA) and β -actin antibodies were from Abcam.

Cell culture and transfection. K562 cells or K562/ADM cells were incubated in RPMI-1640 medium containing 10% fetal calf serum and 100 U/ml penicillin and 100 mg/ml streptomycin (Thermo Fisher Scientific, Inc.) in a 37°C, 5% CO₂ incubator. 5 \times 10⁵ cells/well were seeded into a 6-well plate. When the K562/ADM cell confluency reached >80%, miRNAs, siRNA or overexpression vectors were transfected using Lipofectamin[®]2000 according to the manufacturer's instructions. miRNAs, siRNA or overexpression plasmid vectors (Sangon Biotech Co., Ltd.) were diluted to a final concentration of 100 nM in 250 μ l of FBS-free RPMI-1640 medium and mixed gently. Lipofectamin[®]2000 (5 μ l) was gently mixed, diluted in 250 μ l FBS-free RPMI-1640 medium and incubated for 5 min at room temperature. Following gentle mixing, samples were further incubated for 20 min at room temperature. The DNA/lipofectamine[®]2000 complexes were then added to cells and incubated at 37°C in a CO₂ incubator for 48 h.

Cell proliferation analysis. CCK-8 assay was used to analyze cell proliferation. A total of 24 h after miRNA transfection, cells were seeded in a 96-well plate at a density of 5 \times 10⁴ cells/well. A total of 1, 2, 3 and 4 days after plating, the CCK-8 reagent was added to the cells at a final concentration of 10% and the cells were incubated in a 5%CO₂, 37°C incubator for 2 h. The absorbance at 450 nm was measured and recorded at each time point. Finally, the proliferative curve was analyzed to compare the proliferation rate among groups.

Apoptosis analysis. Apoptosis was evaluated using an Annexin V-FITC/PI cell apoptosis detection kit (Nanjing KeyGen Biotech Co., Ltd.). K562/ADM cells were collected and stained with PI and Annexin V for 15 min at 25°C away from light and tested by a BD flow cytometer (BD Biosciences) and analyzed using FlowJo[™] software version 7.6.5 (FlowJo LLC).

Reverse transcription-qPCR (RT-qPCR). Total RNA was purified by RNAiso Plus reagent. For miRNA quantification, the RNA was reverse transcribed using a miR-18a-5p-specific primer (5'-GTCGTATCCAGTGCAGGGTCCGAGGTA TTCGACTGGATACGAUGGAAU-3') and a U6-specific primer (5'-AACGCTTACGAATTTGCGT-3'). A total of 500 ng RNA, 20 pmol miR-18a-5p-specific primer, 20 pmol U6-specific primer, 4 μ l 5X reaction buffer, 0.5 μ l Ribolock RNase inhibitor, 2 μ l dNTP mix and 1 μ l RevertAid Reverse Transcriptase (Thermo Fisher Scientific, Inc.) were added to a 20 μ l mixture. The temperature protocol of reverse transcription protocol was as follows: 42°C for 60 min, followed by 72°C for 10 min. miRNA quantification was performed using the miRNA qPCR master mix. U6 was used as a reference gene. The qPCR primer pair for miR-18a-5p was as follows:

Forward, GGGGAUAGACGUGAUCUA and reverse, GTG CAGGTCCGAGGT. The primer pair for U6 was as follows: Forward, CTCGCTTCGGCAGCACA and reverse, AACGCT TCACGAATTTGCGT. A total of 10 μ l 2X miRNA qPCR master mix, 0.5 μ l forward primer, 0.5 μ l reverse primer and 2 μ l template were mixed to a total volume of 20 μ l. The thermocycling conditions for PCR were as follows: 95°C for 30 sec; 95°C for 5 sec and 60°C for 30 sec for 40 cycles. HIF-1 α mRNA quantification was performed using 2X SGExel FastSYBR Mixture (Sangon Biotech Co., Ltd.). The RNA was reverse transcribed using the oligo (dT) 15 primer. A total of 500 ng RNA, 20 pmol oligo (dT) 15 primer, 4 μ l 5X reaction buffer, 0.5 μ l Ribolock RNase inhibitor, 2 μ l dNTP mix and 1 μ l RevertAid Reverse Transcriptase were added to a total mixture of 20 μ l. The reverse transcription protocol was as follows: 42°C for 60 min, followed by 72°C for 10 min. β -actin was used as a reference gene. The primer pair for HIF-1 α was as follows: Forward, GGACAAGTCACCACAGGACA and reverse, GGGAGAAAATCAAGTCGTGC. The primer pair for β -actin was as follows: Forward, CACCTTCTACAA TGAGCTGCGTGTG and reverse, ATAGCACAGCCTGGA TAGCAACGTAC. 25 μ l 2 x SGExel FastSYBR Mixture (with ROX), 1 μ l forward primer, 1 μ l reverse primer and 2 μ l template were mixed in 50 μ l mixture. The PCR protocol for mRNA quantification is as follows: 95°C for 20 sec; 95°C for 3 sec and 60°C for 30 sec with 35 cycles. The relative expression of miR-18a-5p and HIF-1 α mRNA was calculated according to the $2^{-\Delta\Delta C_q}$ method (30).

Western blotting. K562/ADM cells were lysed and total proteins were extracted using RIPA buffer with protease and phosphatase inhibitors (Thermo Fisher Scientific, Inc.). Total protein concentration was determined using a BCA protein assay (Thermo Fisher Scientific, Inc.). A total of 20 μ g protein was loaded per lane, separated by 5% SDS-PAGE and transferred to a PVDF membrane. Primary antibodies for targeted molecules were added and incubated at 4°C for 12 h. The following primary antibodies were used (all from Abcam): Caspase-3 and C-Caspase-3 (cat. no. ab13847; 1:200), HIF-1 α (cat. no. ab179483; 1:500), GLUT1 (cat. no. ab115730; 1:200), HK2 (cat. no. ab209847; 1:600), PKM2 (cat. no. ab137852; 1:500), LDHA (cat. no. ab101562; 1:300) and β -actin (cat. no. ab8226; 1:500). A rabbit IgG-HRP antibody (Abcam; cat. no. ab270144; 1:800) was used as the secondary antibody and was incubated at 25°C for 1 h. β -actin antibody (cat. no. ab6276; 1:1,000; Abcam) was used as an internal reference. Membranes were stripped with Restore™ Plus Western Blot Stripping Buffer (Thermo Fisher Scientific, Inc.) for 30 min at room temperature. The blots were re-blocked in 5% w/v milk, 1X TBS + 0.1% v/v Tween-20 at 25°C for 1 h and re-probed. Target protein expression levels were normalized to the β -actin level. The density of respective bands was semi-quantified using a densitometer with Alpha View Software 3.0 (ProteinSimple).

Luciferase reporter assay. The wild type 3'-UTR and mutated 3'-UTR of HIF-1 α were cloned into Dual-Glo Luciferase assay plasmids (Promega Corporation). K562/ADM cells cultured in a 6-well plate were transfected with 1 μ g plasmids and 50 pmol miR-18a-5p mimics or miR-NC using Lipofectamine®2000. The pRL-CMV Renilla luciferase vector

(Promega Corporation) was used to normalize cell numbers and transfection efficiency. After 24 h, the luciferase assay was performed using a luciferase assay kit (Promega Corporation).

ATP analysis. ATP was quantified using an ATP Bioluminescence Assay kit Cls II (Roche Diagnostics) according to the manufacturer's instruction. Briefly, 2x10⁶ K562/ADM cells were collected and mixed with 400 μ l ATP buffer [100 mM Tris, 4 mM EDTA (pH 7.75)] and the mixture incubated at 100°C for 2 min. After centrifugation, the supernatant was collected and the protein was quantified by the BCA assay. Luciferase reagent at a volume of 100 μ l was added into 100- μ l sample. Fluorescence was detected by an ELx808 Absorbance Microplate Reader (BioTek Instruments, Inc.). After subtracting the blank values from the raw data, the ATP concentration was calculated from the standard curve data.

Glucose, lactic acid and pyruvate measurement. For glucose uptake analysis, 2x10⁵ K562/ADM cells were seeded into a 96-well plate 48 h after transfection and further incubated at 37°C in a 5% CO₂ incubator for 48 h. 2-NBDG (Invitrogen; Thermo Fisher Scientific, Inc.) was added into the cells at a final concentration of 5 mM. The cells were incubated for another 15 min at 37°C and the absorbance at 488 nm was recorded and normalized to the cell number. The relative glucose uptake for all groups was expressed as the absorbance value normalized to that of the untreated group.

For lactic acid analysis, 1x10⁵ K562/ADM cells were seeded into a 12-well plate and incubated at 37°C for 10 h. The media were replaced with FBS-free media. After incubation at 37°C for 1 h, the supernatant was collected for lactic acid measurement using a lactate assay kit (BioVision, Inc.) according to the manufacturer's protocol. Absorbance at 450 nm was recorded and normalized to the cell number. The relative lactic acid level was expressed as the absorbance value normalized to that of the untreated group.

For pyruvate analysis, 5x10⁵ K562/ADM cells were treated with Pyruvate Kinase Assay Buffer (BioVision, Inc.). The extract was collected by centrifugation at 3,000 x g at 4°C for 30 min and measured by Pyruvate Kinase Activity Assay kit (BioVision, Inc.) according to the manufacturer's protocol. Absorbance at 570 nm was recorded and normalized to the cell number. The relative pyruvate level was expressed as the absorbance value normalized to that of the untreated group.

Extracellular acidification rate (ECAR) and oxygen consumption rate (OCR) assays. ECAR and OCR were analyzed by Seahorse XF Glycolysis Stress Test kit and Seahorse XF Cell Mito Stress Test kit (Agilent Technologies), respectively, using Seahorse XFe 96 Extracellular Flux Analyzer (Seahorse Bioscience; Agilent Technologies). Transfected cells (1x10⁵) were inoculated into a microplate and incubated at 37°C for 10 h followed by ECAR and OCR tests. For ECAR analysis, glucose, oligomycin (oxidative phosphorylation inhibitor) and 2-DG (glycolytic inhibitor) were added into the cells according to the manufacturer's protocol. For OCR analysis, oligomycin, carbonyl cyanide-4-(trifluoromethoxy)phenylhydrazone (reversible inhibitor of oxidative phosphorylation) and the mitochondrial complex I inhibitor rotenone combined with the

mitochondrial complex III inhibitor antimycin A were sequentially added according to the manufacturer's protocol. Data were analyzed by Seahorse XF96 Wave software (version 2.6; Seahorse Bioscience; Agilent Technologies).

Statistical analysis. Statistical analyses were performed using SPSS software version 16.0 (SPSS, Inc.). Data are presented as the mean \pm standard deviation. Every experiment was carried out independently three times. Statistical significance was evaluated by one-way ANOVA with Turkey's post hoc test. $P < 0.05$ was considered to indicate a statistically significant difference.

Results

miR-18a-5p targets and downregulates HIF-1 α in K562/ADM cells. Using bioinformatics software Targetscan and Miranda, miRNAs that could specifically target HIF-1 α were firstly screened. It was shown that miR-18a-5p has a binding site in the 3'-UTR in HIF-1 α (Fig. 1A). miR-18a-5p expression was further quantified and compared among normal lymphocytes, and K562 and K562/ADM cells by RT-qPCR. miR-18a-5p level was significantly downregulated in K562/ADM cells compared with the K562 cell group and normal lymphocyte group. miR-18a-5p level in K562 cells was significantly lower than that in the normal lymphocyte group, but higher than that in the K562/ADM group (Fig. 1B). Subsequently, miR-18a-5p mimics were transfected into K562/ADM cells and the level of miR-18a-5p increased up to 8-fold compared with that in the miR-NC group (Fig. 1C). In addition, HIF-1 α vector transfection could efficiently upregulate the HIF-1 α mRNA expression level and siHIF-1 α vector transfection could efficiently downregulate the HIF-1 α mRNA expression level in K562/ADM cells (Fig. 1D). Overexpression of miR-18a-5p significantly downregulated HIF-1 α expression on both mRNA (Fig. 1E) and protein levels (Fig. 1F). Luciferase assay showed that miR-18a-5p significantly attenuated the relative luciferase activity of the wild type 3'-UTR construct but not the mutated 3'-UTR construct (Fig. 1G), indicating that miR-18a-5p suppressed HIF-1 α expression by directly targeting the 3'-UTR in HIF-1 α .

miR-18a-5p inhibits proliferation and induces apoptosis of K562/ADM cells by targeting HIF-1 α . The biological effects, including cell proliferation and apoptosis, that miR-18a-5p exerted on K562/ADM cells by targeting HIF-1 α were investigated. As shown in Fig. 2A, transfection with miR-18a-5p mimics or siHIF-1 α markedly inhibited cell proliferation compared with the untreated group, miR-NC group and HIF-1 α overexpressing group. Furthermore, overexpression of HIF-1 α ameliorated the inhibitory effect of miR-18a-5p on cell proliferation. Similarly, both miR-18a-5p mimics and siHIF-1 α efficiently induced cell apoptosis, and restoration of HIF-1 α attenuated the apoptosis induced by miR-18a-5p (Fig. 2B). Accordingly, the expression level of apoptosis-associated protein C-caspase-3 was markedly upregulated by miR-18a-5p and restored by HIF-1 α overexpression (Fig. 2C). The results indicated that HIF-1 α was a target of miR-18a-5p to inhibit proliferation and induce apoptosis of K562/ADM cells.

miR-18a-5p suppresses the warburg effect by targeting HIF-1 α . HIF-1 α has been previously shown to play a key role in the Warburg effect (31). Therefore, it was hypothesized that miR-18a-5p may act as a potential Warburg effect regulator. However, it remained to be elucidated whether miR-18a-5p may participate in aerobic glycolysis in leukemia cells. To analyze the influence of miR-18a-5p on the Warburg effect by targeting HIF-1 α , miR-18a-5p mimics were transfected or co-transfected with HIF-1 α -overexpressing plasmids into K562/ADM cells. miR-18a-5p level was confirmed by RT-qPCR (Fig. 3A) and HIF-1 α protein expression was confirmed by western blotting (Fig. 3B). Glucose uptake, lactate production, pyruvate production and ATP synthesis, which are the characteristics of the Warburg effect, were analyzed after miR-18a-5p mimics, siHIF-1 α or miR-18a-5p mimics/HIF-1 α overexpression vector transfection. The results showed that miR-18a-5p or siHIF-1 α transfection significantly inhibited glucose uptake (Fig. 3C), lactate production (Fig. 3D), pyruvate level (Fig. 3E) and ATP synthesis (Fig. 3F) in K562/ADM cells. However, the effects were reversed by HIF-1 α overexpression. In addition, ECAR was significantly repressed (Fig. 3G) and OCR was significantly decreased (Fig. 3H) by overexpression of miR-18a-5p, indicative of a decreased overall glycolytic flux and an enhanced mitochondrial respiration, respectively. These effects were reversed by HIF-1 α overexpression. Key molecules involved in the Warburg effect, including GLUT1, HK2, PKM2 and LDHA, were also analyzed by western blotting. It was shown that miR-18a-5p mimic transfection inhibited the expression of these molecules (Fig. 3I). The inhibitory effect of miR-18a-5p was abrogated by overexpression of HIF-1 α . It was confirmed by these results that miR-18a-5p could reverse the Warburg effect by targeting HIF-1 α .

miR-18a-5p enhances sensitivity of K562/ADM cells to Adriamycin by reversing the Warburg effect. The Warburg effect was previously shown to be associated with drug resistance (32). The present study aimed to determine whether inhibiting the Warburg effect by miR-18a-5p could improve the sensitivity of K562/ADM cells to Adriamycin. Firstly, the CCK-8 assay was performed to determine cell proliferation. As shown in Fig. 4A, cell proliferation was inhibited significantly by Adriamycin at day 4 and miR-18a-5p at days 3 and 4 compared with the miR-NC group, whereas the combined administration of Adriamycin and miR-18a-5p reduced cell proliferation more significantly at days 2, 3 and 4 compared with miR-18a-5p or Adriamycin alone. In addition, Adriamycin combined with miR-18a-5p resulted in a significantly increased apoptosis rate in K562/ADM cells compared with miR-18a-5p or Adriamycin alone (Fig. 4B). Accordingly, the expression of apoptosis-associated protein C-caspase-3 was markedly upregulated by miR-18a-5p, ADM and miR-18a-5p + ADM, and the level of C-caspase-3 in miR-18a-5p + ADM group was markedly higher than miR-18a-5p and ADM groups (Fig. 4C). These results indicated that miR-18a-5p enhanced the sensitivity of K562/ADM cells to Adriamycin by reversing the Warburg effect.

Discussion

The Warburg effect is a hallmark of cancer cells exhibiting an increased glucose uptake, lactate fermentation, increased

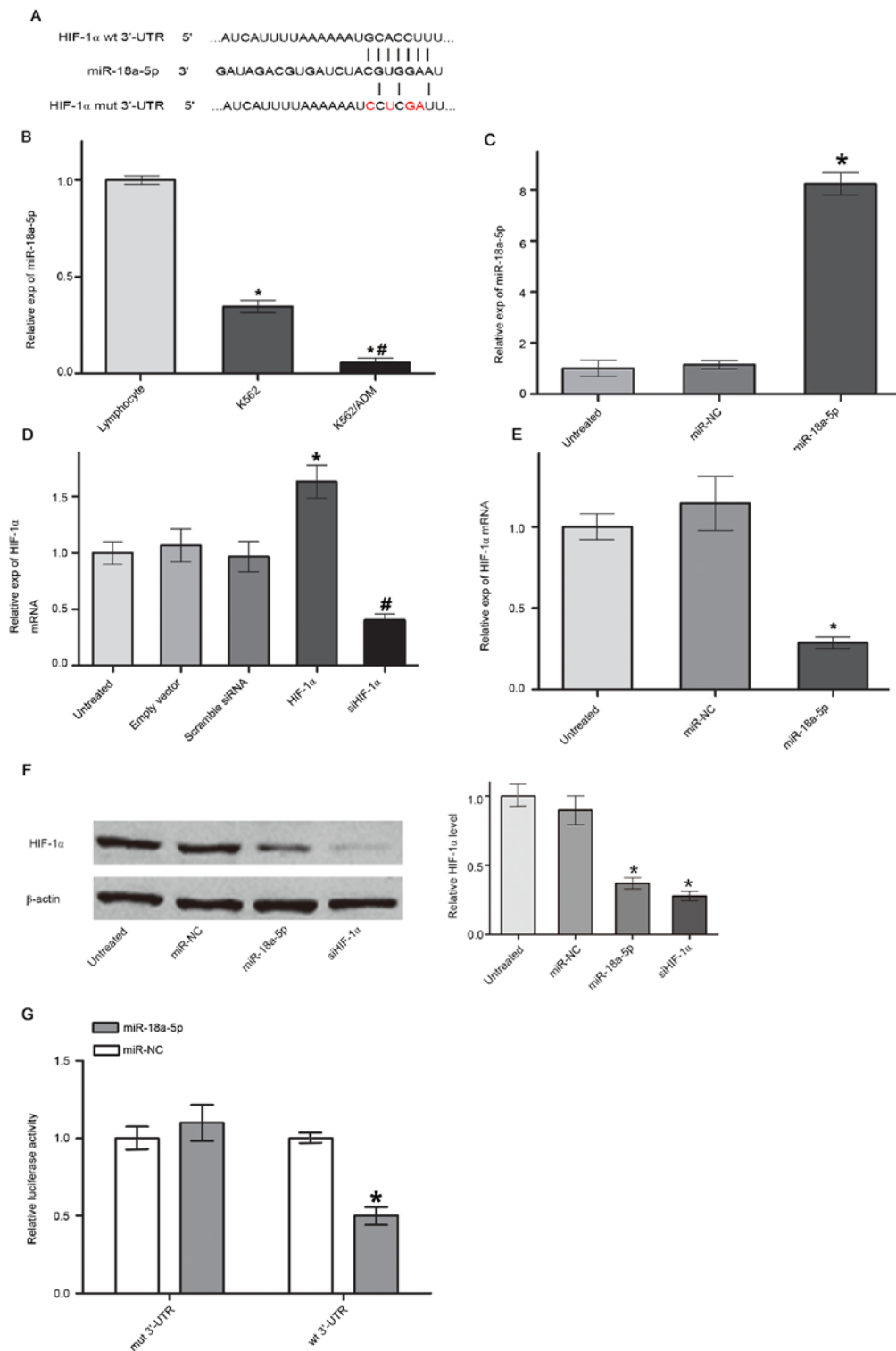


Figure 1. miR-18a-5p downregulates HIF-1 α by binding to the 3'-UTR in HIF-1 α . (A) Binding site of miR-18a-5p to the wt 3'-UTR and mut 3'-UTR in HIF-1 α . The red color denotes the mutated nucleotides. (B) miR-18a-5p level in K562 cells, K562/ADM cells and normal lymphocytes. * P <0.05 vs. lymphocyte; # P <0.01 vs. K562. (C) miR-18a-5p expression levels in K562/ADM cells transfected with miR-NC and miR-18a-5p mimics, quantified by RT-qPCR. * P <0.05 vs. miR-NC. (D) HIF-1 α mRNA expression levels in K562/ADM cells transfected with an empty vector, HIF-1 α , scrambled siRNA and siHIF-1 α , quantified by RT-qPCR. * P <0.05 vs. empty vector; # P <0.05 vs. scrambled siRNA. (E) HIF-1 α mRNA level in K562/ADM cells transfected with miR-NC and miR-18a-5p mimics, evaluated by RT-qPCR. * P <0.05 vs. miR-NC. (F) HIF-1 α protein expression evaluated by western blot analysis and normalized to β -actin. * P <0.05 vs. miR-NC. (G) Luciferase reporter assays of K562/ADM cells co-transfected with mut 3'-UTR plasmids or wt 3'-UTR plasmids and miR-18a-5p mimics or miR-NC. * P <0.05 vs. miR-NC (n=3). miR, microRNA; UTR, untranslated region; mut, mutated; wt, wild-type; HIF-1 α , hypoxia-inducible factor 1 α ; NC, negative control; RT-qPCR, reverse transcription-quantitative PCR; si, small interfering RNA.

glycolysis rate and decreased respiration, even in the presence of oxygen. Using this aberrant metabolic process, cancer cells

can acquire enough energy for proliferation, migration and survival (33). It has been widely recognized that the transcription

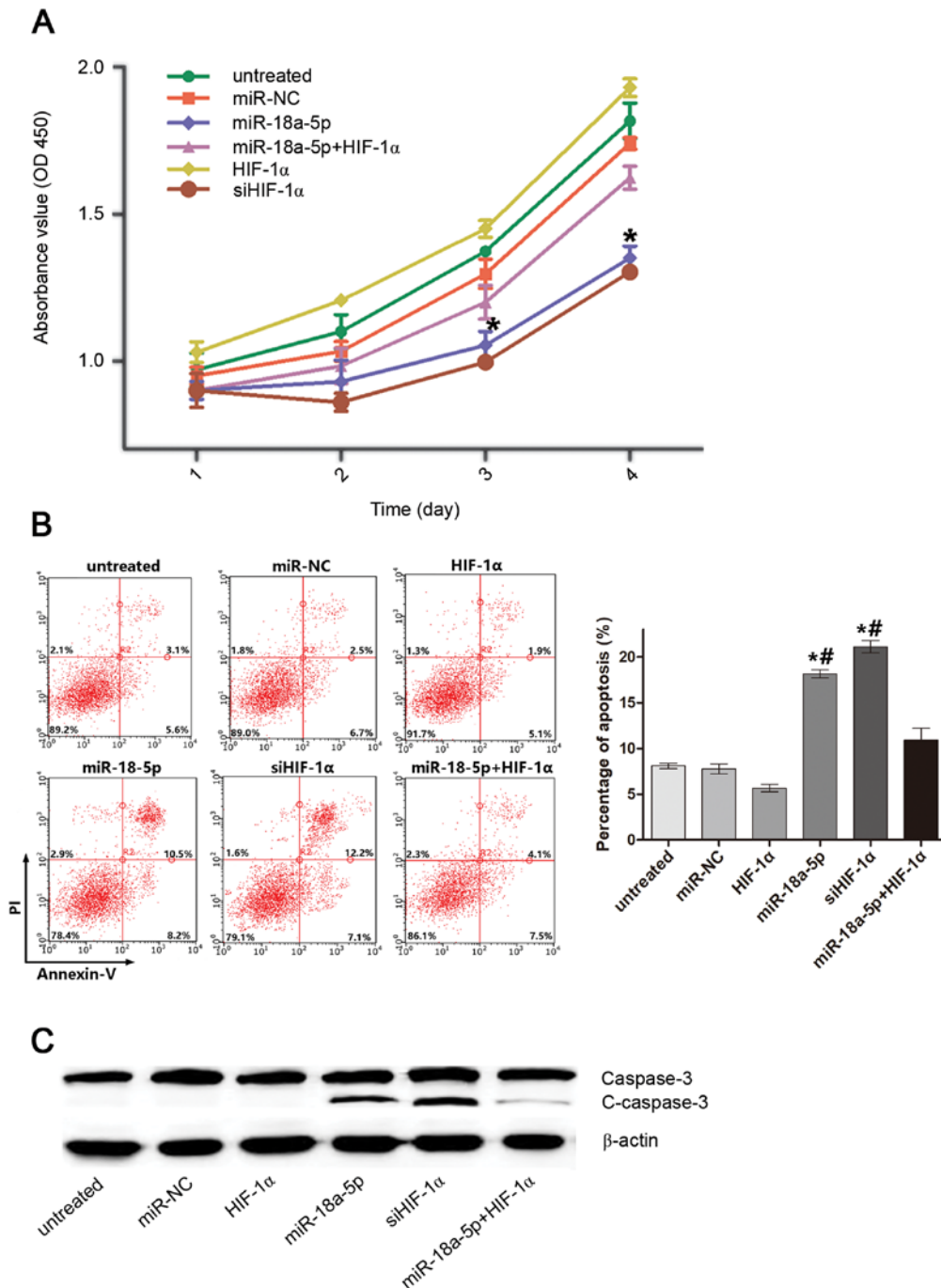


Figure 2. Cell proliferation and apoptosis analysis. (A) Proliferation of K562/ADM cells evaluated by Cell Counting Kit-8 assay. * $P < 0.05$ vs. miR-NC. (B) Apoptosis of K562/ADM cells evaluated by flow cytometry. * $P < 0.05$ vs. miR-NC; # $P < 0.05$ vs. miR-18a-5p + HIF-1 α . $n = 3$. (C) Caspase-3 protein level analyzed by western blotting. miR, microRNA; HIF-1 α , hypoxia-inducible factor 1 α ; c-caspase-3, cleaved caspase-3; NC, negative control; si, small interfering RNA.

factor HIF-1 α plays an essential role in the Warburg effect concerning the glucose uptake, lactate production, pyruvate metabolism and respiration, providing a valuable target for cancer treatment and insight into the mechanism conducive to novel drug discovery (34). The present study investigated the Warburg effect on a cellular level and a strategy of improving the sensitivity of leukemia cells to Adriamycin by targeting HIF-1 α .

miRNAs take part in a series of biological process of cancer cells, including proliferation, differentiation and apoptosis (35). According to the complementary base pairing principle, miRNAs bind and degrade target genes

at the post-transcriptional level (36). An array of miRNAs have been identified to be involved in regulating aerobic glycolysis. For example, miRNAs can inhibit the Warburg effect through targeting the 3'-UTR of LDHA or HK2 (37). Zhu *et al* (38) reported that expression of miRNA-31-5p was positively associated with the Warburg effect in two lung cancer cell lines by specifically targeting HIF-1 α inhibitor mRNA, which indicated the important regulatory role of HIF-1 α in the Warburg effect. In the present study, miR-18a-5p was identified as a direct inhibitor of HIF-1 α . Hence, it was hypothesized that miR-18a-5p may play a

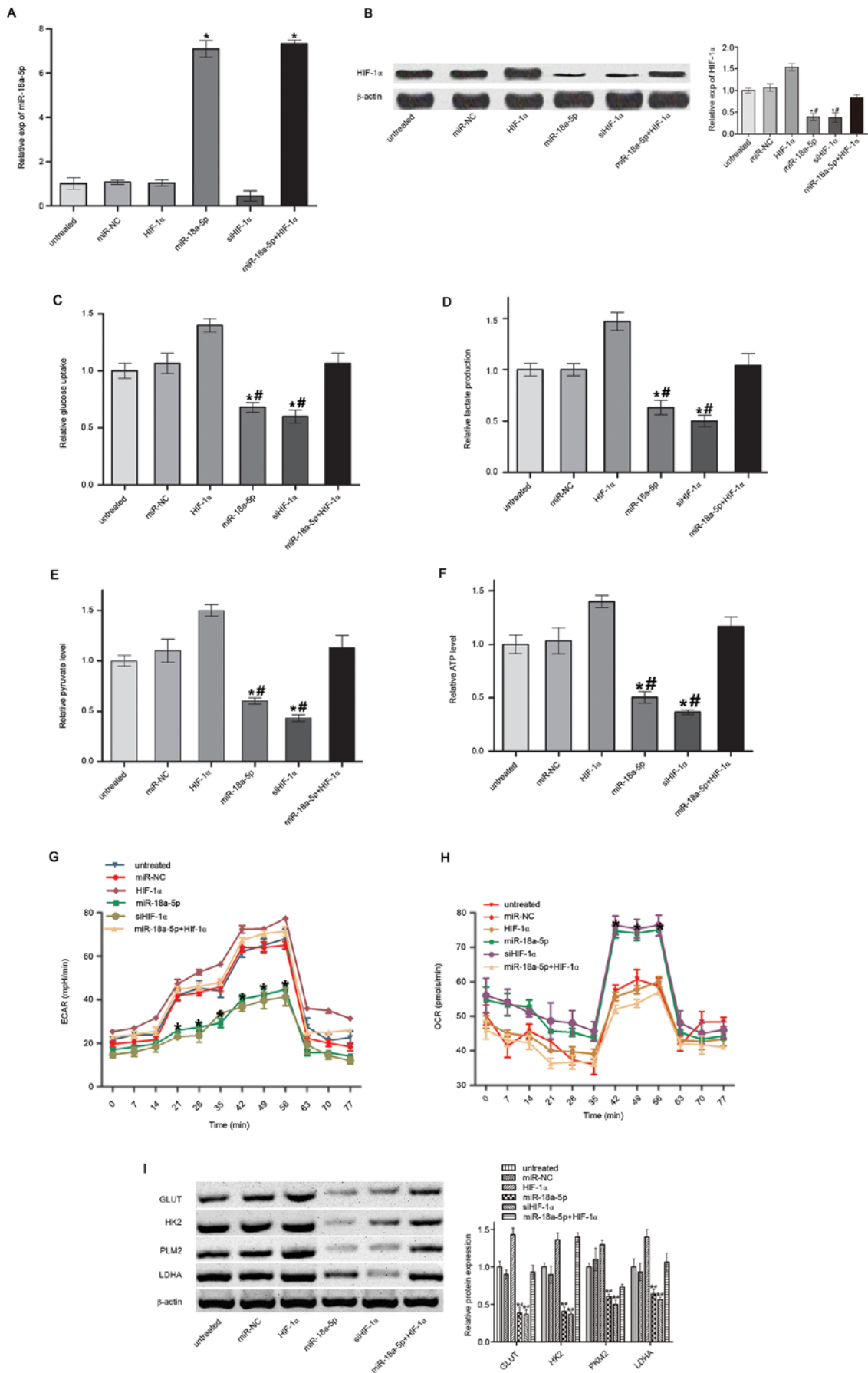


Figure 3. Warburg effect analysis. (A) miR-18a-5p level. (B) HIF-1α protein level. (C) Glucose uptake. (D) Lactate production. (E) Pyruvate level. (F) ATP synthesis. (G) ECAR. (H) OCR. (I) Expression of Warburg effect-associated proteins in K562/ADM cells. *P<0.05 vs. miR-NC; #P<0.05 vs miR-18a-5p + HIF-1α. n=3. miR, microRNA; HIF-1α, hypoxia-inducible factor 1α; NC, negative control; ECAR, extracellular acidification rate; OCR, oxygen consumption rate; GLUT, glucose transporter-1 protein; HK2, hexokinase 2; PKM2, pyruvate kinase M2; LDHA, lactate dehydrogenase A; si, small interfering RNA.

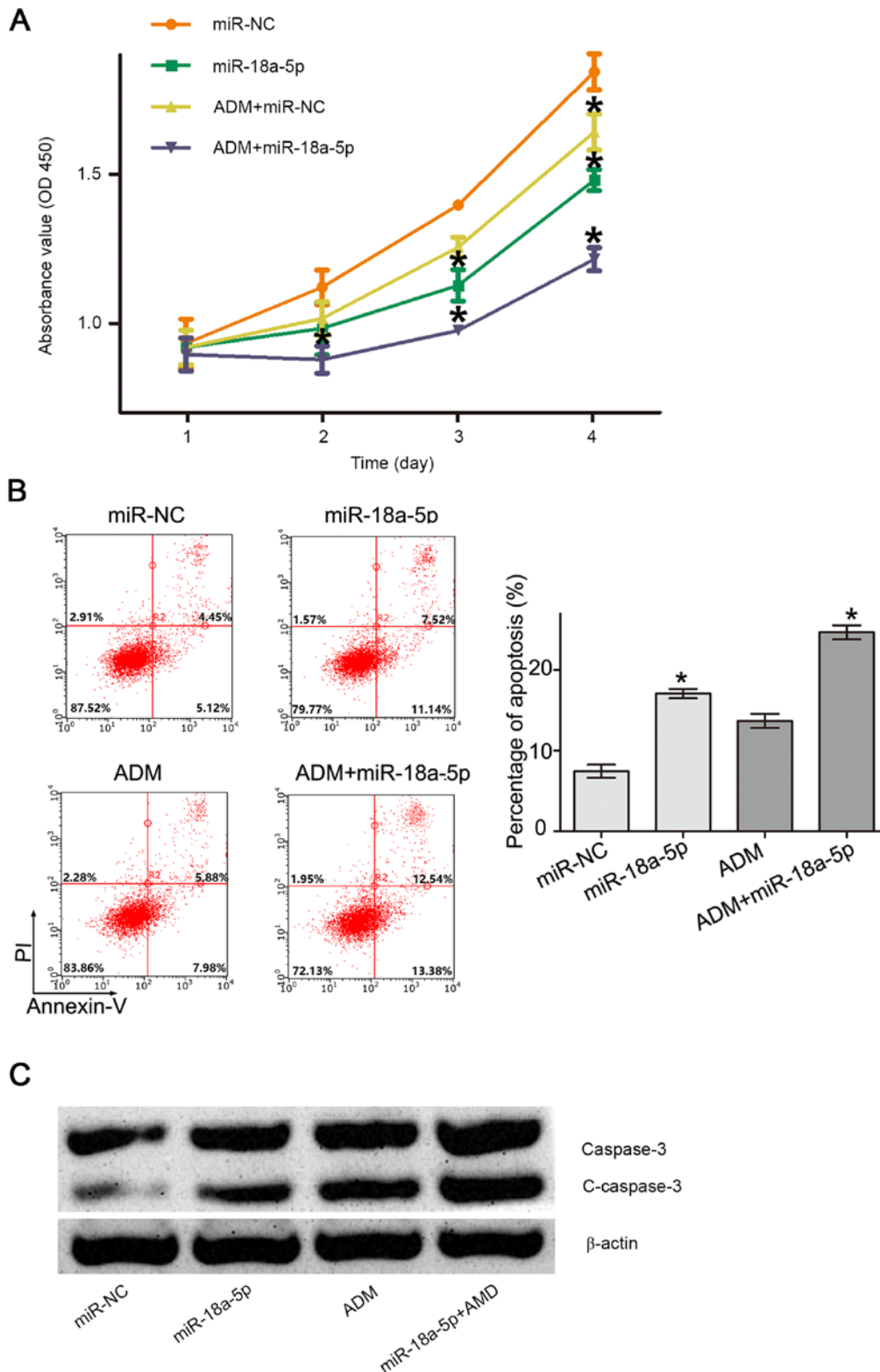


Figure 4. Effect of miR-18a-5p combined with ADM on K562/ADM cells. (A) Proliferation of K562/ADM cells treated with miR-NC, miR-18a-5p, ADM and miR-18a-5p + ADM analyzed by Cell Counting Kit-8. * $P < 0.05$ vs. miR-NC. $n = 3$. (B) Apoptosis of K562/ADM cells treated with miR-NC, miR-18a-5p, ADM and miR-18a-5p + ADM analyzed by flow cytometry. * $P < 0.05$ vs. miR-NC. $n = 3$. (C) Caspase-3 protein level analyzed by western blot analysis. ADM, Adriamycin; miR, microRNA; NC, negative control; c-caspase-3, cleaved caspase-3.

functional role in the Warburg effect. Aberrant expression of miR-18a-5p has been observed in cancer cell lines and tumor tissues, and its regulatory mechanism may be varied in different types of cancer. In HCT116 colon cancer cells, miR-18a-5p can upregulate autophagy and ataxia

telangiectasia mutated gene, with the potential for colon cancer inhibition (39). However, miR-18a-5p is upregulated in non-small cell lung cancer (NSCLC) tissues and NSCLC cell lines and functions as an oncogene by directly targeting interferon regulatory factor 2 (28). Downregulating

miR-18a-5p using long non-coding RNA FENDRR also inhibits prostate cancer progression (29).

The present study demonstrated that the level of miR-18a-5p in the K562/ADM cell line was significantly lower than that in the normal lymphocytes, indicating that miR-18a-5p may act as a suppressor in CML. Bioinformatics analysis revealed that HIF-1 α may be a potential target of miR-18a-5p. The miR-18a-5p expression level in K562/ADM cells was significantly downregulated compared with that in the K562 cells and normal lymphocytes. However, the miR-18a-5p expression level in K562 cells was relatively high compared with that in K562/ADM cells. The function of miR-18a-5p in K562 cells, which is a limitation of the present study, will be explored in our future work. The present study indicated that the mRNA and protein levels of HIF-1 α can be decreased by miR-18a-5p overexpression. Transfection of miR-18a-5p mimics inhibited cell proliferation and induced apoptosis in K562/ADM cells, and restoration of HIF-1 α expression reversed the biological effects of miR-18a-5p. The above results indicated that miR-18a-5p can inhibit K562/ADM cells by targeting HIF-1 α . The Warburg effect associated with miR-18a-5p was further explored in the present study. miR-18a-5p could inhibit the ATP level, glucose uptake, lactate production and pyruvate level in K562/ADM cells. ECAR and OCR assays were performed to analyze the overall glycolytic flux and mitochondrial oxidative respiration changes (40,41). The results revealed that ECAR was decreased and OCR was enhanced by miR-18a-5p mimics. Furthermore, expression of downstream molecules of HIF-1 α , including GLUT1, HK2, PKM2 and LDHA, which are closely associated with the Warburg effect, was affected by miR-18a-5p transfection. However, overexpression of HIF-1 α could counteract the effects on the Warburg effect exerted by miR-18a-5p mimics. The results indicated that miR-18a-5p was able to inhibit the Warburg effect by targeting HIF-1 α . The Warburg effect has been shown to be involved in drug resistance by increasing drug efflux, DNA damage repair, drug inactivation, and epigenetic alterations or mutations in drug targets (42). Therapeutic strategies, such as RNA interference targeting the Warburg effect combined with chemotherapeutic drugs, are expected to combat chemoresistance of tumors. The present study aimed to sensitize K562/ADM cells, which are commonly utilized as the MDR CML cell model, to Adriamycin using miR-18a-5p mimics. The results suggested that miR-18a-5p combined with Adriamycin significantly inhibited proliferation and induced apoptosis of K562/ADM cells.

In conclusion, the present study demonstrated that miR-18a-5p can suppress the Warburg effect by downregulating HIF-1 α in K562/ADM cells, revealing a novel regulatory mechanism of miR-18a-5p and providing potential targets for CML treatment. Further studies will analyze the relationship between miR-18a-5p and clinical leukemia samples and explore the therapeutic application of miR-18a-5p in an animal model.

Acknowledgements

Not applicable.

Funding

The present study was supported by the Joint Special Fund of Yunnan Province (grant no. 2017FE468), and Health

Science and Technology Program of Yunnan Province (grant nos. 2016NS047 and 2018NS0129).

Availability of data and materials

All data generated or analyzed during this study are included in this published article.

Authors' contributions

KW and YZ conceived and designed the study. SJC, CG and YZ analyzed and interpreted the data, and drafted the manuscript. YXL, BN, JRY, QZ, SJC and YHL performed the experiments. All authors participated in the writing and revision of the manuscript. YZ and BN supervised the project. All authors read and approved the final manuscript. KW and CG confirm the authenticity of all the raw data.

Ethics approval and consent to participate

Not applicable.

Patient consent for publication

Not applicable.

Competing interests

The authors declare that they have no competing interests.

References

- Zhang B, Li L, Ho Y, Li M, Marcucci G, Tong W and Bhatia R: Heterogeneity of leukemia-initiating capacity of chronic myelogenous leukemia stem cells. *J Clin Invest* 126: 975-991, 2016.
- Valera ET, Scrideli CA, Queiroz RG, Mori BM and Tone LG: Multiple drug resistance protein (MDR-1), multidrug resistance-related protein (MRP) and lung resistance protein (LRP) gene expression in childhood acute lymphoblastic leukemia. *Sao Paulo Med J* 122: 166-171, 2004.
- O'Hare T, Corbin AS and Druker BJ: Targeted cml therapy: Controlling drug resistance, seeking cure. *Curr Opin Genet Dev* 16: 92-99, 2006.
- Gora-Tybor J: Emerging therapies in chronic myeloid leukemia. *Curr Cancer Drug Targets* 12: 458-470, 2012.
- Baccarani M, Deininger MW, Rosti G, Hochhaus A, Soverini S, Apperley JF, Cervantes F, Clark RE, Cortes JE, Guilhot F, *et al*: European LeukemiaNet recommendations for the management of chronic myeloid leukemia: 2013. *Blood* 122: 872-884, 2013.
- Luqmani YA: Mechanisms of drug resistance in cancer chemotherapy. *Med Prin Pract* 14 (Suppl 1): S35-S48, 2005.
- Wang X, Chen B, Zhao L, Zhi D, Hai Y, Song P, Li Y, Xie Q, Inam U, Wu Z, *et al*: Autophagy enhanced antitumor effect in k562 and k562/ADM cells using realgar transforming solution. *Biomed Pharmacother* 98: 252-264, 2018.
- Dyshlovoy SA, Pelageev DN, Hauschild J, Borisova KL, Kaune M, Krisp C, Venz S, Sabutskii YE, Khmelevskaya EA, Busenbender T, *et al*: Successful targeting of the warburg effect in prostate cancer by glucose-conjugated 1,4-Naphthoquinones. *Cancers (Basel)* 11: 1690, 2019.
- Koppenol WH, Bounds PL and Dang CV: Otto Warburg's contributions to current concepts of cancer metabolism. *Nat Rev Cancer* 11: 325-337, 2011.
- Liberti MV and Locasale JW: The warburg effect: How does it benefit cancer cells? *Trends Biochem Sci* 41: 211-218, 2016.
- Bhattacharya B, Mohd Omar MF and Soong R: The warburg effect and drug resistance. *Br J Pharmacol* 173: 970-979, 2016.

12. Li L, Liang Y, Kang L, Liu Y, Gao S, Chen S, Li Y, You W, Dong Q, Hong T, *et al.*: Transcriptional regulation of the warburg effect in cancer by six1. *Cancer Cell* 33: 368-385.e7, 2018.
13. Ni Z, He J, Wu Y, Hu C, Dai X, Yan X, Li B, Li X, Xiong H, Li Y, *et al.*: Akt-mediated phosphorylation of ATG4B impairs mitochondrial activity and enhances the warburg effect in hepatocellular carcinoma cells. *Autophagy* 14: 685-701, 2018.
14. Fu D, Li J, Wei J, Zhang Z, Luo Y, Tan H and Ren C: HMGB2 is associated with malignancy and regulates Warburg effect by targeting LDHB and FBP1 in breast cancer. *Cell Commun Signal* 16: 8, 2018.
15. de Andrade Barreto E, de Souza Santos PT, Bergmann A, de Oliveira IM, Wernersbach Pinto L, Blanco T, Rossini A, Pinto Kruel CD, Mattos Albano R and Ribeiro Pinto LF: Alterations in glucose metabolism proteins responsible for the warburg effect in esophageal squamous cell carcinoma. *Exp Mol Pathol* 101: 66-73, 2016.
16. Hanahan D and Weinberg RA: Hallmarks of cancer: The next generation. *Cell* 144: 646-674, 2011.
17. Barnes K, Mcintosh E, Whetton AD, Daley GQ, Bentley J and Baldwin SA: Chronic myeloid leukaemia: An investigation into the role of Bcr-Abl-induced abnormalities in glucose transport regulation. *Oncogene* 24: 3257-3267, 2005.
18. Wang YH and Scadden DT: Targeting the warburg effect for leukemia therapy: Magnitude matters. *Mol Cell Oncol* 2: e981988, 2015.
19. Brittain EL: Clinical trials targeting metabolism in pulmonary arterial hypertension. *Adv Pulm Hypertens* 17: 110-114, 2018.
20. Yeung SJ, Pan J and Lee MH: Roles of p53, MYC and HIF-1 in regulating glycolysis-the seventh hallmark of cancer. *Cell Mol Life Sci* 65: 3981-3999, 2008.
21. Szakács G, Paterson JK, Ludwig JA, Booth-Genthe C and Gottesman MM: Targeting multidrug resistance in cancer. *Nat Rev Drug Discov* 5: 219-234, 2006.
22. Zhu W, Huang Y, Pan Q, Xiang P, Xie N and Yu H: MicroRNA-98 suppress warburg effect by targeting HK2 in colon cancer cells. *Dig Dis Sci* 62: 660-668, 2016.
23. Zhang S, Pei M, Li Z, Li H, Liu Y and Li J: Double-negative feedback interaction between DNA methyltransferase 3A and microRNA-145 in the warburg effect of ovarian cancer cells. *Cancer Sci* 109: 2734-2745, 2018.
24. Fathollahzadeh S, Mirzaei H, Honardoost MA, Sahebkar A and Salehi M: Circulating microRNA-192 as a diagnostic biomarker in human chronic lymphocytic leukemia. *Cancer Gene Ther* 23: 327-332, 2016.
25. Ichihara A, Wang Z, Jinnin M, Izuno Y, Shimozone N, Yamane K, Fujisawa A, Moriya C, Fukushima S, Inoue Y and Ihn H: Upregulation of miR-18a-5p contributes to epidermal necrolysis in severe drug eruptions. *J Allergy Clin Immunol* 133: 1065-1074, 2014.
26. Xu XL, Jiang YH, Feng JG, Su D, Chen PC and Mao WM: MicroRNA-17, microRNA-18a, and microRNA-19a are prognostic indicators in esophageal squamous cell carcinoma. *Ann Thorac Surg* 97: 1037-1045, 2014.
27. Takakura S, Mitsutake N, Nakashima M, Namba H, Saenko VA, Rogounovitch TI, Nakazawa Y, Hayashi T, Ohtsuru A and Yamashita S: Oncogenic role of miR-17-92 cluster in anaplastic thyroid cancer cells. *Cancer Sci* 99: 1147-1154, 2008.
28. Liang C, Zhang X, Wang HM, Liu XM, Zhang XJ, Zheng B, Qian GR and Ma ZL: MicroRNA-18a-5p functions as an oncogene by directly targeting IRF2 in lung cancer. *Cell Death Dis* 8: e2764, 2107.
29. Zhang G, Han G, Zhang X, Yu Q, Li Z, Li Z and Li J: Long non-coding RNA FENRRR reduces prostate cancer malignancy by competitively binding miR-18a-5p with RUNX1. *Biomarkers* 23: 435-445, 2018.
30. Livak KJ and Schmittgen TD: Analysis of relative gene expression data using real-time quantitative PCR and the 2(-Delta Delta C(T)) method. *Methods* 25: 402-408, 2001.
31. Li B, He L, Zuo D, He W, Wang Y, Zhang Y, Liu W and Yuan Y: Mutual Regulation of MiR-199a-5p and HIF-1 α modulates the warburg effect in hepatocellular carcinoma. *J Cancer* 8: 940-949, 2017.
32. Icard P, Shulman S, Farhat D, Steyaert JM, Alifano M and Lincet H: How the Warburg effect supports aggressiveness and drug resistance of cancer cells? *Drug Resist Updates* 38: 1-11, 2018.
33. Lévy P and Bartosch B: Metabolic reprogramming: A hallmark of viral oncogenesis. *Oncogene* 35: 4155-4164, 2015.
34. Semenza GL: HIF-1 mediates the warburg effect in clear cell renal carcinoma. *J Bioenerg Biomembr* 39: 231-234, 2007.
35. Rothschild SI: microRNA therapies in cancer. *Mol Cell Ther* 2: 7, 2014.
36. Agarwal V, Bell GW, Nam JW and Bartel DP: Predicting effective microRNA target sites in mammalian mRNAs. *Elife* 4: e05005, 2015.
37. Li L, Kang L, Zhao W, Feng Y, Liu W, Wang T, Mai H, Huang J, Chen S, Liang Y, *et al.*: miR-30a-5p suppresses breast tumor growth and metastasis through inhibition of LDHA-mediated Warburg effect. *Cancer Lett* 400: 89-98, 2017.
38. Zhu B, Cao X, Zhang W, Pan G, Yi Q, Zhong W and Yan D: MicroRNA-31-5p enhances the Warburg effect via targeting FIH. *FASEB J* 33: 545-556, 2019.
39. Qased AB, Yi H, Liang N, Ma S, Qiao S and Liu X: MicroRNA-18a upregulates autophagy and ataxia telangiectasia mutated gene expression in HCT116 colon cancer cells. *Mol Med Rep* 7: 559-564, 2012.
40. Faubert B, Boily G, Izreig S, Griss T, Samborska B, Dong Z, Dupuy F, Chambers C, Fuerth BJ, Viollet B, *et al.*: AMPK is a negative regulator of the warburg effect and suppresses tumor growth in vivo. *Cell Metab* 17: 113-124, 2013.
41. Xian S, Shang D, Kong G and Tian Y: FOXJ1 promotes bladder cancer cell growth and regulates Warburg effect. *Biochem Biophys Res Commun* 495: 988-994, 2017.
42. Raz S, Sheban D, Gonen N, Stark M, Berman B and Assaraf YG: Severe hypoxia induces complete antifolate resistance in carcinoma cells due to cell cycle arrest. *Cell Death Dis* 5: e1067, 2014.



This work is licensed under a Creative Commons Attribution-NonCommercial-NoDerivatives 4.0 International (CC BY-NC-ND 4.0) License.